

Proceedings of the Korean Nuclear Society Autumn Meeting

Suwon, Korea, October 2001

Cell Based CMFD Formulation for Acceleration of Whole-core Method of Characteristics Calculations

Jin Young Cho, Han Gyu Joo, Kang Seog Kim, and Sung Quun Zee

Korea Atomic Energy Research Institute

P.O.Box 105, Yuseong, 305-353,

Daejeon, Korea

Abstract

This paper is to apply the well-established coarse mesh finite difference(CMFD) method to the method of characteristics(MOC) transport calculation as an acceleration scheme. The CMFD problem is first formulated at the pin-cell level with the multi-group structure. To solve the cell-based multi-group CMFD problem efficiently, a two-group CMFD formulation is also derived from the multi-group CMFD formulation. The performance of the CMFD acceleration is examined for three test problems with different sizes including a realistic quarter core PWR problem. The CMFD formulation provides a significant reduction in the number of ray tracings and thus only about 10 ray tracing iterations are enough for the realistic problem. In computing time, the CMFD accelerated case is about two-three times faster than the coarse-mesh rebalancing(CMR) accelerated case.

1. Introduction

For whole-core transport calculations, the method of characteristics (MOC) is known to be adequate because of the easy handling of heterogeneous pin cell geometry via ray tracing. Iterative ray tracing eliminates the need for constructing a matrix that couples various regions in the domain as needed in the collision probability method. One of the merits of MOC is therefore the simplicity of not dealing with a large linear system. Similar to S_n methods, the angles are discretized in MOC, and the solution accuracy can be adjusted by choosing the number of angles and ray spacing. However, the convergence rate of MOC is very poor and an acceleration scheme is essential for practical applications. In some of the earlier work, the coarse mesh rebalancing(CMR) method was used for the acceleration of MOC calculations.^{1,2} The results showed that speedups of about 5 to 10 were attainable with the CMR acceleration in the MOC transport calculations.

The coarse mesh finite difference (CMFD) formulation is widely used as an efficient implementation of the advanced nodal method.^{3,4} In this formulation, current correction coefficients are iteratively determined at each node interface by higher order nodal

calculations. Using the current correction coefficient, it is possible to formulate a transport equivalent fine-mesh diffusion problem as Smith employed for the acceleration of the CASMO4 MOC transport calculation.⁵ In general, the CMFD method showed a convergence feature of 2 or 3 times faster than the CMR method in solving eigenvalue problems.

In the work here, a two-level CMFD formulation is developed as an alternative acceleration scheme for MOC based whole-core transport calculations and its performance is examined against the CMR scheme. The first level is the multi-group CMFD formulation based on heterogeneous cell cross sections and MOC transport solutions. The second level is the two-group CMFD formulation based on the multi-group CMFD formulation and the neutron spectrum of each cell. In this two-level CMFD formulation, the multigroup MOC calculations are accelerated by the multigroup CMFD calculations which are further accelerated by the two-group CMFD calculations. For this work, a prototype whole-core MOC code named DeCART (Deterministic transport based on CMFD Accelerated Ray Tracing) has been written. In the following section, the features of the DeCART MOC solver are described first. In Section 3, the multi-group and two-group CMFD formulations are derived. In Section 4, the iteration algorithm for alternate MOC transport calculation and the CMFD diffusion calculation is described. In Section 5, the performance of CMFD acceleration is examined with the focus on the convergence feature and the computational time.

2. Features of the DeCART MOC Solver

One of the crucial components of an MOC solver is the modular ray tracing module. In DeCART, a cell-based modular ray-tracing module was established instead of assembly based modular ray tracing for the purpose of saving memory as well as programming effort. Another feature of the DeCART MOC solver is a computational technique to reduce the overhead associated with the evaluation of exponential functions. The two features of the DeCART MOC solver are described below.

2.1 Cell Based Modular Ray Tracing

Generation of all the ray segments for the whole core geometry requires enormous computational memory and programming effort. To avoid this problem, the ray segments are generated only for each cell type and the rays defined for each cell are linked to the rays of the adjacent nodes through path linking. For path linking, each ray must align itself exactly with its reflective counterpart at the cell boundary. To meet this condition, the ray spacing and azimuthal angle are adjusted from the evenly spaced initial angles and uniform ray spacing determined by the input parameters.⁶ Specifically, the adjusted azimuthal angles and ray spacing are determined as:

$$\tan(\mathbf{j}_a) = \frac{N_{a,x}}{N_{a,y}} \quad (1)$$

and

$$dA_a = \frac{P}{\sqrt{N_{a,x}^2 + N_{a,y}^2}} \quad (2)$$

where

$$N_{a,x} = \text{int}\left(\frac{P}{d\tilde{A}}|\sin(\tilde{\mathbf{j}}_a)|\right), \text{ and } N_{a,y} = \text{int}\left(\frac{P}{d\tilde{A}}|\cos(\tilde{\mathbf{j}}_a)|\right).$$

In the above equation, $\tilde{\mathbf{j}}_a$ are the evenly spaced azimuthal angles which are determined from the user input for the number of azimuthal angles, and $d\tilde{A}$ and P mean the ray spacing and cell pitch, respectively. The “int()” indicates the ceiling function which determines the greatest integer lower than or equal to its arguments. In the choice of the polar angles and their weights, the optimal values suggested by Leonard and McDaniel⁷ are used.

2.2 Approximation of the Exponential Function

The outgoing angular flux in the MOC transport calculation is expressed in terms of incoming angular flux and the regional angular flux source as:

$$\mathbf{y}_{o,m}^k = \left(\mathbf{y}_{i,m}^k - \frac{Q_m^k}{\Sigma_{tr}^k} \right) e^{-\frac{\mathbf{t}_m^k}{\sin q_m}} + \frac{Q_m^k}{\Sigma_{tr}^k} \quad (3)$$

where $\mathbf{y}_{i,m}^k$, $\mathbf{y}_{o,m}^k$ are the incoming and outgoing angular fluxes in the direction Ω_m at region k . Since this expression has to be evaluated for each ray segment, the exponential function is called very frequently in the iterative MOC calculation and it takes most of the MOC computational time to compute the exponential value. In DeCART, the exponential values are pre-calculated and stored as a piecewise linear function using a table form. With this exponential table, a 60% reduction in the MOC computational time was possible.

3. Pin-Cell Based CMFD Formulation

Using the CMFD formulation, it is possible to construct a pin-cell based diffusion problem which is equivalent to the MOC transport calculation with finer regions defined. In the formulation of the CMFD diffusion problem, cell homogenized constants and current correction coefficients are required. In this section, the cell homogenization and the calculation of current correction coefficients are described first, and then the method for the utilizing of the CMFD solution in the subsequent MOC transport calculation is established. Note that the CMFD solution would accelerate the convergence of the fission and scattering

source terms in the MOC calculation.

3.1 Cell Homogenized Multi-Group Constants and Multi-Group CMFD Calculation

The cell homogenized multi-group constants can be calculated from the heterogeneous regional cross-sections and scalar fluxes as follows:

$$\bar{\Sigma}_{xg}^i = \frac{\sum_{k \in i} V^k \Sigma_{xg}^k \mathbf{f}_g^k}{\bar{\mathbf{f}}_g^i V^i} \quad (4)$$

and

$$\bar{D}_g^i = \frac{\bar{\mathbf{f}}_g^i V^i}{3 \sum_{k \in i} V^k \Sigma_{trg}^k \mathbf{f}_g^k} \quad (5)$$

where

$$\bar{\mathbf{f}}_g^i = \frac{\sum_{k \in i} V^k \mathbf{f}_g^k}{V^i} \quad \text{and} \quad V^i = \sum_{k \in i} V^k .$$

In the above equation, \mathbf{f}_g^k is the scalar flux of region k that is determined from the MOC transport calculation.

The current correction coefficient can be calculated from the cell surface average current, cell average fluxes and cell homogenized diffusion constant by:

$$\hat{D}_g^i = - \frac{j_g^i + \tilde{D}_g^i (\bar{\mathbf{f}}_g^{i+1} - \bar{\mathbf{f}}_g^i)}{\bar{\mathbf{f}}_g^{i+1} + \bar{\mathbf{f}}_g^i} \quad (6)$$

where \tilde{D}_g^i is the nodal coupling coefficient determined in the ordinary finite difference method and j_g^i the cell surface average current determined from the MOC transport result by:

$$j_g^i = \sum_{m \in i} w^m \mathbf{y}_{g,m}^i . \quad (7)$$

With the cell homogenized group constants and the current correction coefficients defined above, multigroup CMFD calculations can be performed and the result of the CMFD calculation will be cell average scalar fluxes. Since the subsequent MOC transport calculation

requires updated regional scalar fluxes and core boundary angular fluxes from the CMFD calculation, the regional scalar fluxes are updated by using the previous shape, namely:

$$\mathbf{f}_g^{k,l+\frac{1}{2}} = \frac{\mathbf{f}_g^{k,l}}{\bar{\mathbf{f}}_g^{i,l}} \bar{\mathbf{f}}_g^{i,l+\frac{1}{2}} \quad (8)$$

where l is the iteration index. Similarly, the angular fluxes at the core boundaries can be updated by:

$$\mathbf{y}_{g,m}^{i,l+\frac{1}{2}} = \frac{\mathbf{y}_{g,m}^{i,l}}{j_g^{i,l}} (\tilde{D}_g^i - \hat{D}_g^i) \bar{\mathbf{f}}_g^{i,l+\frac{1}{2}}. \quad (9)$$

3.2 Two-Group Constants and Two-Group CMFD Calculation

The two-group based CMFD formulation is well-established in the nodal diffusion code as MASTER⁸ or PARCS³, and successfully applied to accelerate multi-group diffusion calculation.⁹ A two-group CMFD formulation is thus employed here to accelerate the multi-group CMFD solution.

The two-group constants are simply calculated using multi-group constants and multi-group spectra as follows:

$$\bar{\Sigma}_{xG}^i = \sum_{g' \in G} \bar{\Sigma}_{xg'}^i \bar{f}_{g'}^i \quad (10)$$

and

$$\bar{D}_G^i = \frac{1}{\sum_{g' \in G} \frac{\bar{f}_{g'}^i}{\bar{D}_{g'}^i}} \quad (11)$$

where G is the energy group index in the two-group CMFD equation and \bar{f}_g^i is the neutron spectrum which is defined as:

$$\bar{f}_g^i = \frac{\mathbf{f}_g^i}{\sum_{g' \in G} \mathbf{f}_{g'}^i}. \quad (12)$$

To calculate the current correction coefficient, condensed two-group surface currents are required, which can be calculated using the results of the multi-group CMFD calculation. The multi-group surface currents are determined from the multi-group CMFD solution by:

$$j_g^i = -\tilde{D}_g^i (\bar{F}_g^{i+1} - \bar{F}_g^i) - \hat{D}_g^i (\bar{F}_g^{i+1} + \bar{F}_g^i). \quad (13)$$

Then the condensed two-group surface currents are calculated by summing the multi-group currents as:

$$J_G^i = \sum_{g \in G} j_g^i. \quad (14)$$

In the calculation of the two-group current correction coefficients, Eq. (6) is used as in the multi-group case.

Once a two-group CMFD solution is obtained, the multi-group scalar fluxes have to be established by prolongation of the two-group scalar fluxes. The prolongation can be achieved simply by multiplying the two-group scalar fluxes and the multi-group spectrum of Eq. (12).

4. Iterative Algorithm of Pin-Cell Based CMFD and MOC Method

Fig 1. shows the iteration algorithm to obtain a converged solution in the pin-cell CMFD accelerated MOC method. First, the homogenized multi-group cross sections for all cells and current correction coefficients at cell interfaces are calculated. The two-group cross sections and current correction coefficients are determined from the multi-group cross sections and multi-group corrective coupling coefficients by using the multi-group spectra. The CMFD calculation begins from the two-group calculation and moves to the multi-group calculation if the error reduction criteria are satisfied. The multi-group CMFD calculation continues until the error reduction is satisfied or the number of iterations meets the user input. After the multi-group CMFD calculation is completed, the need for an MOC transport update is determined using the two-group CMFD error reduction. The alternate two-group and multi-group CMFD calculations continue until the error reduction condition on the MOC update is met. In general, about 3 or 4 alternate CMFD iterations are required to advance to the MOC transport calculation. This is because the error reduction criterion for the MOC update is tighter than that of the multi-group CMFD calculation.

If the flag for advancing to the MOC transport calculation is turned on, the multi-group scalar fluxes for heterogeneous cells and multi-group angular fluxes at the core boundaries are updated using Eqs. (8) and (9). The fission sources are then calculated at all regions using the updated multi-group scalar fluxes. One MOC transport calculation is completed by performing ray tracing once or twice - twice for the first two iterations. The ray tracing is performed for each group given the fission and scattering sources. In the group sweep, one or two up-scattering iterations are performed - two for the first 4 ray tracings. During the ray tracing, the contribution of each ray to the incoming and outgoing partial currents at the cell interfaces is accumulated for the calculation of the current correction coefficients. After the MOC transport calculation is finished, the new fission sources are calculated at all regions and the overall convergence is checked using the fission sources. If the convergence is not met, another pin-cell based CMFD calculation is invoked.

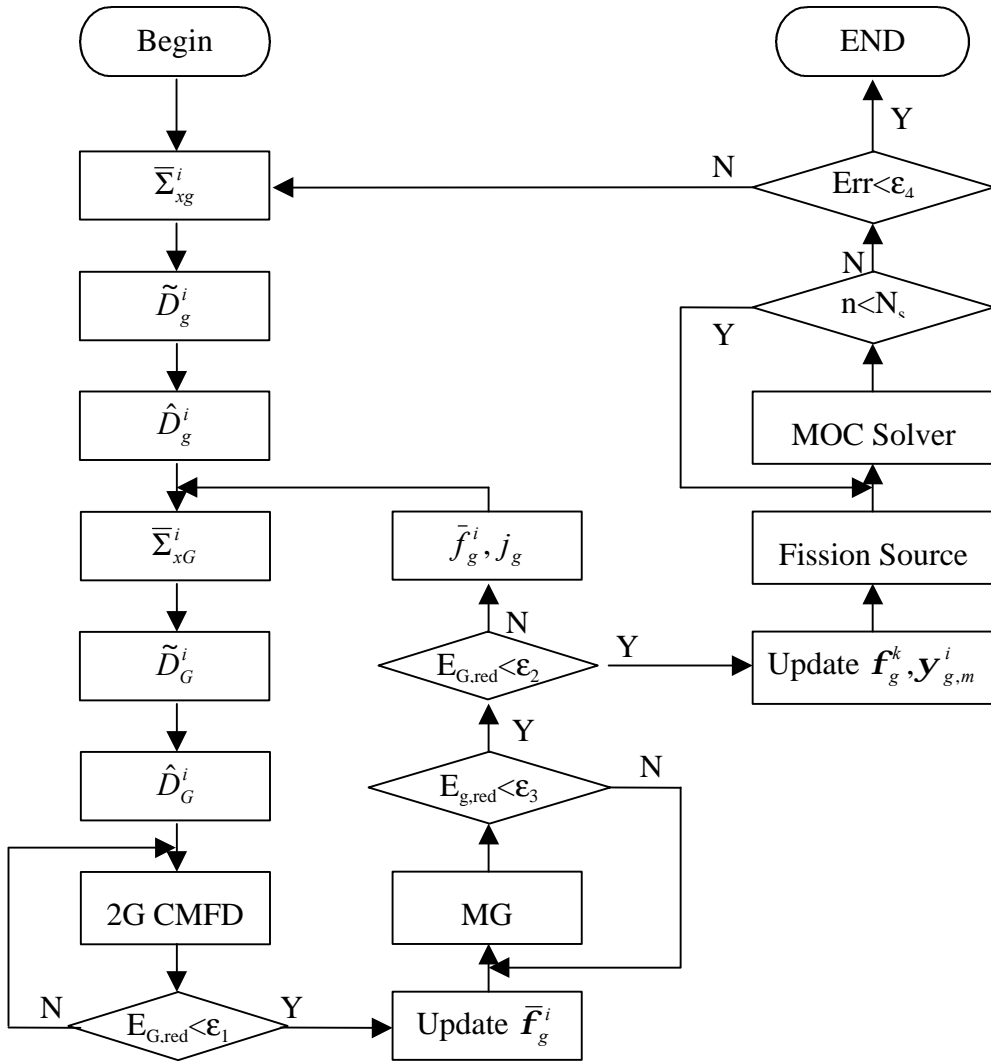


Figure 1. Iterative Algorithm of Two-Level CMFD Accelerated MOC Method

5. Performance Examination

In order to examine the convergence characteristics of the pin-cell based CMFD formulation, DeCART is applied to three test problems: an assembly problem with reflective boundary condition, KAIST benchmark problem 2A¹⁰ and a realistic quarter core problem with 81 assemblies. The performance of the CMFD acceleration is compared against the power iteration using Chebyshev two-parameter extrapolation and pin-cell based CMR acceleration. The fuel, burnable absorber, control rod and guide tube cells are divided into 48 regions, and baffle and reflector cells are divided into 4 regions. In this examination, the 7-group cross section sets of KAIST benchmark problem 2A are used. To examine the

convergence characteristics, a reference solution is generated for each problem with a very tight convergence criterion and the error of each iterate is calculated as the difference from the reference solution.

5.1 Assembly Problem

The assembly problem is for the MOX fuel assembly with 8 burnable absorber rods. The user input values for the number of azimuthal angles on 180 degree and ray spacing are 16 and 0.3 mm, respectively. Figure 2 shows the fission source error reduction behavior with the MOC ray tracing numbers. The number of the CMFD accelerated ray tracings is only 7, which is about 2.5 times and 6 times fewer than that of the CMR accelerated ray tracing and the Chebyshev extrapolated power iteration, respectively. As shown in Table 1, the reduction in the number of ray tracings is reflected in the computing time. The CMFD case is about 2 times faster than the CMR case.

5.2 KAIST Benchmark Problem 2A

The core of the KAIST benchmark problem is composed of various fuel assemblies including MOX and uranium fuel assemblies. The user input values for the number of azimuthal angles and ray spacing are 8 and 0.3 mm, respectively. Figure 3 shows the fission source error reduction behavior. The number of the CMFD case is 9, which is about 2.5 times and 10 times fewer than that of the CMR and the Chebyshev cases, respectively. Table 1 shows the computational time breakups. The saving in the computing time is also about two as in the assembly problem.

5.3 Realistic Core Problem

This problem is to examine the applicability of the MOC whole core calculation to the realistic core. The quadrant core is constructed with 52 fuel and 29 reflector assemblies. The fuel assemblies are selected from the KAIST benchmark 2A problem. Figure 4 shows the fuel loading pattern of this problem. The user input values for the number of azimuthal angles and ray spacing are 8 and 0.3 mm, respectively. As shown in Figure 5, the error reduction characteristic of the CMFD case is superior compared to the CMR and Chebyshev cases. The number of ray tracings is only 9 in the CMFD case, resulting in reduction factors of 3 and 55 for the CMR and the Chebyshev cases, respectively. The reduction in the computing time by a factor of 2.5 is remarkable in this realistic problem.

6. Conclusion

In this paper, the well-established CMFD formulation is applied to the whole-core MOC transport calculation. The computational results show that the CMFD formulation reduces the number of ray tracings by a factor of 6-55 compared with the Chebyshev two-parameter extrapolation and 2-3 compared with the CMR acceleration method. Consequently, the

CMFD formulation provides a speedup of 2.5 in computing time over the CMR acceleration method. These results indicate that the CMFD acceleration is very effective in whole core MOC transport calculations.

ACKNOWLEDGEMENT

This work was performed under the long-term nuclear research and development program sponsored by Ministry of Science and Technology of Korea.

Reference

1. G. S. Lee, N. J. Cho and S. G. Hong, "Acceleration and Parallelization of the Method of Characteristics for Lattice and Whole-Core Heterogeneous Calculation," ANS Int. Topical Meeting on Advances in Reactor Physics and Mathematics and Computation into the next Millennium, PHYSOR 2000, Pittsburgh, Pennsylvania, May 7-12, 2000.
2. S. Kosaka and E. Saji, "The Characteristics Transport Calculation for a Multi-Assembly System using Neutron Path Linking Technique," Proc. Int. Conf. Mathematics and Computation, Reactor Physics and Environmental Analysis in Nuclear Applications, p. 1890, Madrid, Spain, Sep. 27-30, 1999.
3. H. G. Joo, G. Jiang and T. J. Downar, "Stabilization Techniques for the Nonlinear Analytic Nodal Method," Nucl. Sci. Eng, 130, 47, 1998.
4. Y. A. Chao, "Coarse Mesh Finite Difference Methods and Applications," ANS Int. Topical Meeting on Advances in Reactor Physics and Mathematics and Computation into the next Millennium, PHYSOR 2000, Pittsburgh, Pennsylvania, May 7-12, 2000.
5. K. S. Smith and J. D. Rhodes III, "CASMO Characteristics Methods for Two-Dimensional PWR and BWR Core Calculations," Trans. Am. Nucl. Soc., Winter Mtg., Washington D. C., 294-296, 2000.
6. M. J. Halsall, "CACTUS, A Characteristics Solution to the Neutron Transport Equations in Complicated Geometries," AEEW-R-1291, United Kingdom Atomic Energy Authority, Winfrith, 1980.
7. A. Leonard, C. T. McDaniel, "Optimal Polar Angles and Weights for the Characteristics Method," Trans. Am. Nucl. Soc., 73, 172, 1995.

8. H. G. Joo et. al., "One-Node Solution Based Nonlinear Analytic Nodal Method," Proceedings of the Korean Nuclear Society Autumn Meeting., Pohang, Korea, May 26-27, 2000.
9. H. G. Joo, J. Y. Cho, J. S. Song, and S. Q. Zee, "Multigroup Transient Calculation within the Framework of a Two-Group Hexagonal CMFD Formulation," The '2001 ANS. Mtg. Math. Method. Nucl. Appl., Salt Lake City, UT, Sept. 9-13, 2001.
10. N. Z. Cho, "Benchmark Problems in Reactor and Particle Transport Physics," available on internet (<http://nurapt.kaist.ac.kr/benchmark>>) (June 2000).

Table 1. Computational Time Breakup(1 GHz PENTIUM III PC, sec)

Prob.	Chebyshev Extrap.		CMR Acceleration			CMFD Acceleration		
	MOC(Nt)*	Total	MOC(Nt)	CMR	Total	MOC(Nt)	CMFD	Total
Assy.	172.6(41)	174.9	81.5(17)	1.4	84.2	39.3(7)	0.6	40.9
KAIST	11303(305)	11511	903(22)	91	1007	417(9)	47	472
PWR	82631(515)	84031	4994(28)	494	5535	1832(9)	131	2003

* The Total Number of MOC Iterations

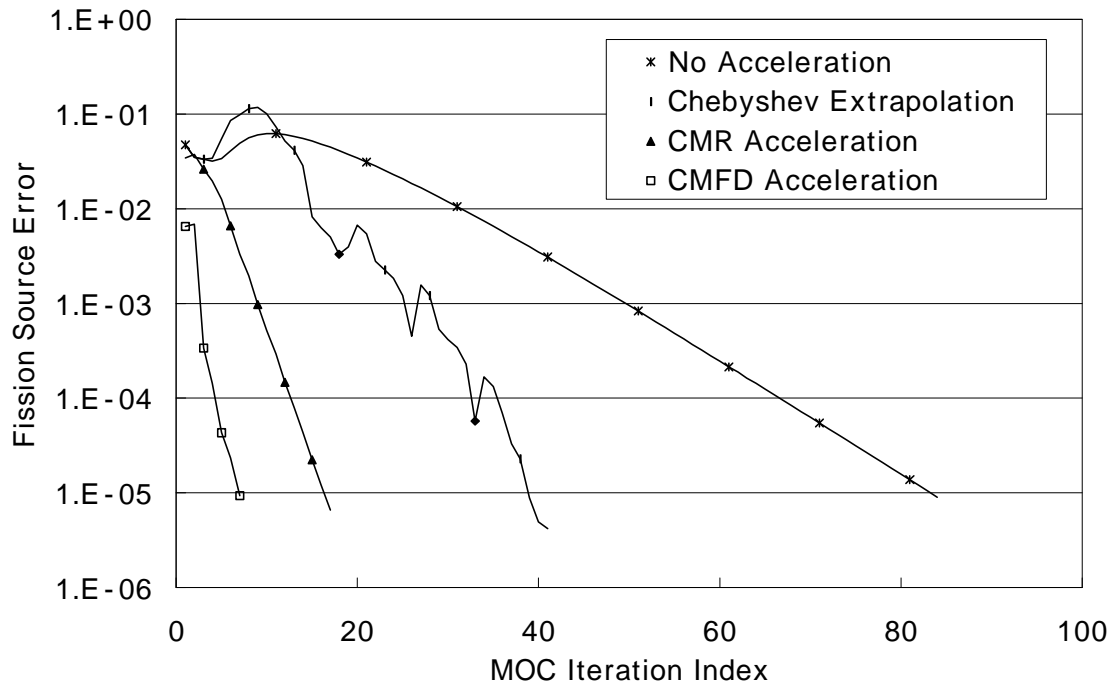


Figure 2. Fission Source Errors for Assembly Problem

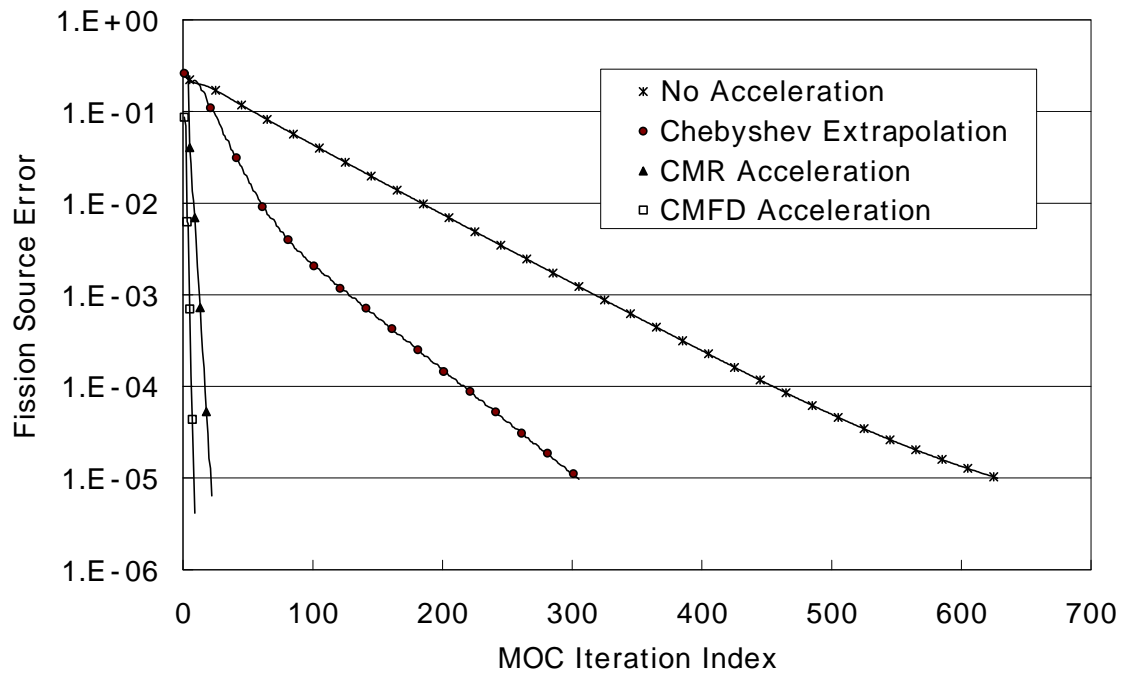


Figure 3. Fission Source Errors for KAIST Benchmark Problem 2A

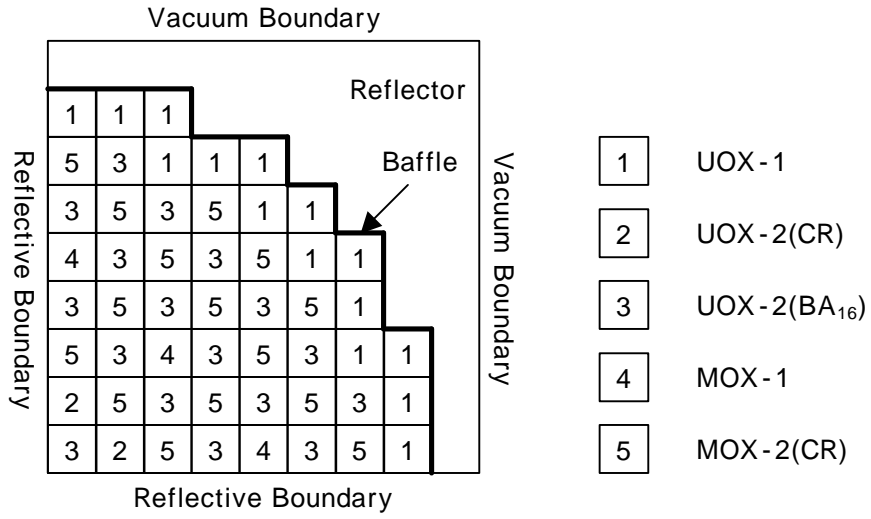


Figure 4. Fuel Loading Pattern for Realistic Core Problem

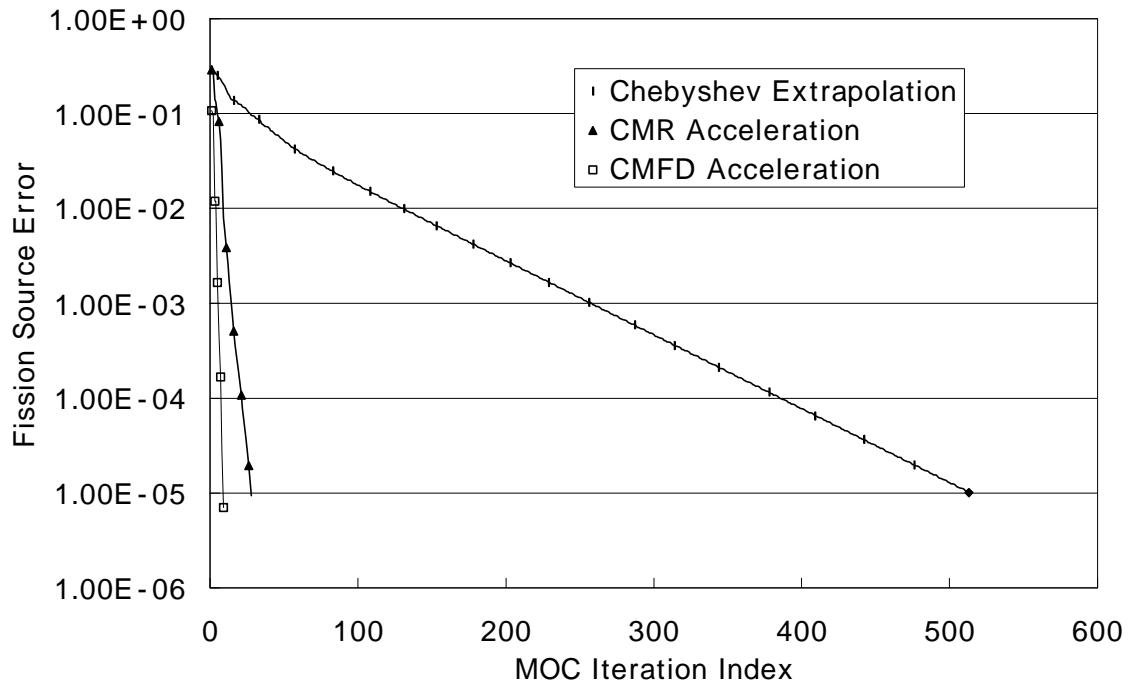


Figure 5. Fission Source Errors for Realistic Core Problem